Vibrational Excitation of H_2 by Proton Impact*

F. A. Herrero and J. P. Doering
Department of Chemistry, Johns Hopkins University, Baltimore, Maryland 21218
(Received 16 September 1971)

The forward-scattered component of the absolute cross sections for proton- and deuteron-impact excitation of the first four vibrational levels of the electronic ground state of H_2 have been measured. Excitation cross-section measurements are reported for laboratory energies from 100 to 1500 eV; and, for energies below 100 eV, excitation cross sections are reported for forward-scattered protons from $\theta = 0°$ to $\theta = 1.9°$. The cross sections were measured from the peak intensities observed in the ion energy-loss spectra generated by passing a high-quality proton beam (energy spread < 80 meV, angular divergence $\leq \pm 1°$) through a collision chamber containing the target gas at room temperature. Each excitation cross section ($\sigma_{0v'}$, where the quantum number v' refers to the final energy level) is found to reach a maximum value at an energy which decreases with increasing quantum number v': $\sigma_{01}(\max) = 1.37 \times 10^{-16}$ cm^2 at 200 eV, $\sigma_{02}(\max) = 0.342 \times 10^{-16}$ cm^2 at 140 eV, and $\sigma_{03}(\max) = 0.078 \times 10^{-16}$ cm^2 and $\sigma_{04}(\max) = 0.021 \times 10^{-16}$ cm^2 both at 110 eV. These maxima give collision times and distances which are consistent with the adiabatic hypothesis. For energies beyond the maxima, the cross sections decrease very slowly with increasing energy. Furthermore, the cross sections for excitation to the higher levels decrease more rapidly than the cross sections for excitation to the lower levels, an effect predicted by Shin in a three-dimensional calculation involving a semiclassical theory for the excitation of a classical harmonic oscillator. A comparison of our results with vibrational excitation studies of other systems demonstrates the unique features of the H^+-H_2 system. The large values of these vibrational excitation cross sections and their wide effective kinetic energy span show that vibrational excitation must be an important process in a wide variety of physical phenomena.

I. INTRODUCTION

It has recently been learned that proton-impact excitation of vibrational transitions within the H_2 electronic ground state occurs with very large cross sections at energies of a few hundred eV.[1] We have now measured the forward-scattered component of the absolute cross sections for proton-impact excitation of the first four vibrational levels of $X^1\Sigma_g^+$ H_2. This paper presents the results of our measurements and a discussion of their significance.

The importance of the proton-H_2 system need hardly be emphasized from the point of view of the physics and chemistry of molecular interactions. This is perhaps the simplest system in which molecular interactions can be observed since only one of the colliding partners can be excited—the other one is structureless with regard to excitation of internal energy levels. The molecule H_2 also provides an ideal target for excitation experiments from a theoretical, as well as experimental, point of view. H_2 is the molecule with the least number of electrons in which close range inelastic collisions can occur at low energies; a simpler quantum-mechanical system would be $H^+ + H_2^+$, but here the entire encounter would be dominated by the repulsive Coulomb barrier, and the character of the excitation would be expected to be very different.[2]

The theoretical treatment of vibrational excitation to date has been devoted almost exclusively to the collinear collision problem.[3] However, a few publications on the solution of the three-dimensional problem have appeared recently.[4–6] Of these, the most pertinent is an extension of a semiclassical theory[7] for the excitation of a classical harmonic oscillator in which the interaction potential of the projectile-target system is a three dimensionally adapted Lennard-Jones potential.[6] Such a simple potential is not realistic for ion-molecule collisions of the type investigated here, and hence, quantitative agreement between this theory and experiment is not expected. It is expected, however, that the theory should account for the salient features of the excitation process, particularly those features which result from the attractive part of the potential.

In principle, the experimental results given here can be used to obtain information about the interaction potential of the projectile-target system. However, at present, the only way that this can be reasonably accomplished is to propose an adequate interaction potential, and then calculate the excitation cross sections using a suitable theory, such as the semiclassical theory mentioned above.[6] A comparison of the calculated cross sections with the experimental results would then give a test of the adequacy of the potential and the reliability of the theory. A careful comparison of the vibrational

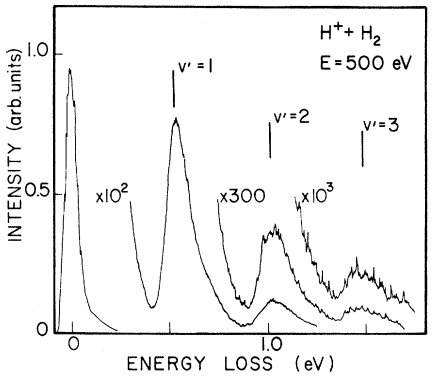

FIG. 1. Energy-loss spectrum of 500-eV protons incident on H_2 gas. Target-gas pressure was approximately 70 mTorr. The lines indicate the locations of the first three vibrational energy levels as known spectroscopically.

excitation cross sections obtained with different interaction potentials has been made,[8] and the results indicate that vibrational excitation is very sensitive to the form of the interaction potential. Thus, a comparison between experiment and theory concerning these processes should provide a very sensitive test of the adequacy of *a priori* interaction potentials.

The potential surface of H_3^+ has been calculated by many authors,[9] but to this date there has been little interest in using such results to calculate excitation transition probabilities. It is hoped that the results presented in this paper will provide some stimulus for the calculation of excitation cross sections.

From the experimental point of view, it is convenient to study the excitation of H_2 because of the large vibrational spacing of this molecule (0.516, 1.004, 1.462, and 1.990 eV for the energy levels of the first four vibrational levels measured from the vibrational ground state).[10] Vibrational excitation by ion impact has been observed in other diatomic molecules with closer vibrational spacing,[11,12] and the character of the excitations is much different from that observed in the $H^+ + H_2$ system.

For purposes which will be indicated below, an investigation of the system $D^+ + H_2$ was carried out, and those results are presented here also.

II. EXPERIMENTAL METHOD

Because the ion spectrometer employed in this experiment has been already described,[13] only a brief discussion of the parts relevant to this experiment will be given.

The excitation cross sections reported here were obtained from the relative intensities of the various components of an energy-loss spectrum generated by passing a proton beam of well-defined energy through the target gas. The energy-loss spectra obtained at many different energies exhibit peaks at energy losses corresponding very closely to the vibrational spacing of the $X^1\Sigma_g^+$ ground state of H_2. One of these spectra is shown in Fig. 1. The first peak on the left-hand side corresponds to the unscattered portion of the primary beam, and the three peaks on the right-hand side correspond to excitation to the first three vibrational levels of H_2. The vertical lines indicate the location of the vibrational levels of H_2.[10]

The ion spectrometer consists of two identical 120° electrostatic spherical analyzers. One is placed before the collision chamber to provide a high-quality proton beam (energy spread $\leq$ 80 meV and angular divergence $\leq \pm 1°$) from the mass-analyzed proton beam of a duoplasmatron ion source. The second analyzer is used to scan the energy-loss spectrum of the beam transmitted through the target gas in the collision chamber. All ions are transmitted through the scattered-particle analyzer at the same energy by the use of a very weak lens which adds back the energy lost in the collision chamber. The voltage applied to this adder lens is a direct measure of the energy loss.

Detection was carried out with an electron multiplier whose output current was measured with a Keithley 602 electrometer. The energy-loss spectra were generated on an x-y recorder in which the x axis was driven by the energy add voltage applied to the scattered particle analyzer, and the y axis was driven by the output of the detector.

The target gas pressure in the collision chamber was measured with an MKS Baratron model 77H manometer.

The beam was collimated at the entrance of the first analyzer by choosing the entrance pupil of the electron optical system small enough to give the desired divergence at the collision chamber.[13] This method of collimation was necessary because of lack of space within the vacuum chamber. The disadvantage of such a technique is that the divergence of the beam in the collision chamber is a function of the incident energy and becomes large enough to cause the beam to begin to strike the collision chamber exit slit walls at energies below about 80 eV (see discussion involving Fig. 2 below).

A. Apparatus Performance

In order for the relative intensities of the different energy components of an energy-loss spectrum to be directly proportional to the excitation cross sections for the various energy levels excited, it is necessary (a) that the transmission of the analyzer be independent of ion energy, and (b) that all the ions within the acceptance cone of the detector be transmitted with equal efficiency.

The first of the above requirements was met by the use of the adder lens in the analyzer which ensured that there was no energy discrimination in the transmitted ions.[13]

A critical examination was made of the effect of angular divergence on transmission. For this purpose a Faraday cup and a deflection plate were installed inside the collision chamber in such a way that the ions entering the collision chamber could be collected in the Faraday cup by applying a positive voltage to the deflector plate. The inside dimensions of the Faraday cup were 1.25 $\times$1.91$\times$7.62 cm deep, so that secondary electrons from the inside of the Faraday cup were effectively trapped. In addition, the ion current was measured without amplification at the first dynode of the electron multiplier detector.[14] The ratio of the detector current to the current measured in the collision chamber is the transmission T of the analyzer system. This quantity is plotted in Fig. 2 as a function of ion energy. A smooth line drawn between the points of measured transmission exhibits a knee at approximately 80 eV of energy. At roughly the same energy, it was noticed that the angular width of the primary beam began to increase as the energy was decreased further below 80 eV. This indicated that either the beam divergence was outside the limits set by the acceptance cone of the detector or that the detector was beginning to discriminate against the more widely divergent components of the beam. The collision chamber exit slit diam was $D = 0.152$ cm, and its distance from the entrance slit was 3.835 cm. These numbers indicate that when the beam divergence exceeds $\pm 1.1°$, the ions will begin to strike the slit walls. Indeed, at this point, the beam cross-sectional diameter is equal to the exit slit diam and the observed angular distribution is given by the convolution of two circles of equal diam D. The distribution normalized to unity is given by

$$\tfrac{1}{4}[\,2\cos^{-1}(r/D) - (2r/D)(1 - r^2/D^2)^{1/2}]\,D^2\,,$$

where r is the distance between the centers of the two circles.[15] In this case r is dependent on the detector angle and is given by $r = R\theta$, where $R = 1.89$ cm is the collision chamber radius and θ is the detector angle given in arc radians. The angle at which the distribution drops to one-half is $\theta_{1/2} = 0.4\,D/R = 1.84°$ which is reasonably close to the experimentally measured value of 1.9° (see Fig. 3). Thus, it can be safely assumed that the drop in transmission at 80 eV is caused by masking

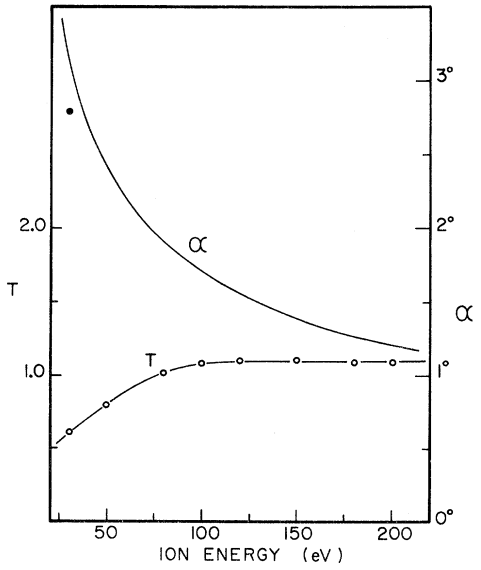

FIG. 2. Dependence of scattered-particle analyzer transmission T on ion energy and illustration of the dependence of beam divergence half-angle α as a function of ion energy according to the Helmholtz-Lagrange law. The transmission remained constant for energies higher than 200 eV. • is the observed half-width at half-maximum at 30 eV.

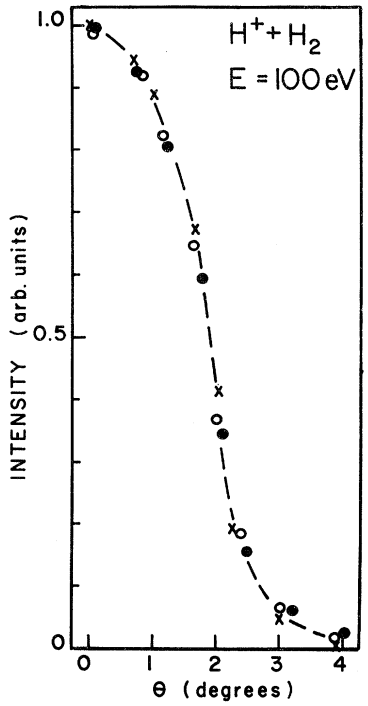

FIG. 3. Angular distributions of elastically and inelastically scattered protons with H_2 gas in the collision chamber. × is the angular distribution corresponding to both the primary beam (no target gas in the collision chamber) and to the elastic scattering (with target gas in the collision chamber). O is the inelastic scattering with excitation to $v' = 1$ vibrational level of H_2; • is the inelastic scattering with excitation to the $v' = 2$ vibrational level of H_2. At 100 eV all scattered particles are well within the acceptance cone of the detector.

of the beam by the exit slit of the collision chamber and not by discrimination against divergent ions. Because the transmission begins to decrease at approximately 100 eV, any measurements taken at energies below 100 eV are valid as long as care is taken to point out that the angle of acceptance of the detector is $\pm 1.9°$. In Fig. 2, a plot of the angular divergence α versus energy indicates how beam divergence is expected to behave on the basis of the Helmholtz-Lagrange law.[16] The curve has been normalized to $1.9°$ at $E = 80$ eV. The point below the curve indicates the measured half-angle at 30 eV laboratory energy. At higher energies the beam divergence is always less than $1.9°$ as shown in Fig. 2, but since the angle of acceptance is now larger than the beam divergence, the observed angular distribution is determined mainly by the angle of acceptance and remains essentially constant at $3.8°$ full width at half-maximum ($\pm 1.9°$ half-angle for the cone of acceptance).

B. Cross-Section Measurement

In obtaining a relation which gives the excitation cross sections in terms of the relative peaks of the energy-loss spectra, it is convenient to consider the attenuation of an ion beam as it passes through a gas which can remove ions from the beam through many different processes. In this case, the only processes which need to be considered are elastic scattering, charge transfer, and vibrational excitation from the ground state to the v'th level. Denoting the respective attenuation coefficients by Q_e, Q_c, and $Q_{0v'}$, the intensity of the beam, after traversing a path of length x in the gas, is given by

$$I = I' \exp\left(-\sum_{v'} Q_{0v'} x\right), \tag{1}$$

where

$$I' = I_0 \exp[-(Q_e + Q_c)x], \tag{2}$$

and I_0 is the beam intensity at $x = 0$. The attenuation coefficient Q is related to the cross section σ by

$$Q = \sigma n, \tag{3}$$

where n is the target gas density.

If $I_{v''}$ is the beam intensity *not* including the attenuation due to excitation to the v''th level, then the portion of the beam which excites the target gas to the v''th level is

$$\Delta I_{v''} = I_{v''} - I = I' \exp\left(-\sum_{v' \neq v''} Q_{0v'} x\right) - I' \exp\left(-\sum_{v'} Q_{0v'} x\right). \tag{4}$$

If it is assumed that the net attenuation due to vibrational excitation is kept small by maintaining a low target-gas pressure, then it follows that

$$\begin{aligned} \Delta I_{v''} &= I'\left(1 - \sum_{v' \neq v''} Q_{0v'} x - 1 + \sum_{v'} Q_{0v'} x\right), \\ \Delta I_{v''} &= I' Q_{0v''} x, \end{aligned} \tag{5}$$

and, substituting relation (3) into Eq. (5), one obtains

$$\sigma_{0v'} = (\Delta I_{v'}/I')(1/xn). \tag{6}$$

With this relation, it is possible to obtain the cross-section values directly from the relative intensities on the energy-loss spectrum. $\Delta I_{v'}$ is the peak intensity corresponding to excitation of the v'th level as measured on the spectrum, and I' is the sum of all the peak intensities in the spectrum. x is the collision path length ($x = 3.835$ cm) and n is the target-gas density. Although it is desirable to keep the attenuation of the beam to a minimum, the target-gas pressure must be brought up to a value high enough to give an adequate signal in the excitation channels of interest. It was found that the neighborhood of 0.70 mTorr of H_2 gas pressure gave an optimum signal throughout the entire energy range studied. Measurements such as the ones shown in Fig. 4 were made at several energies giving essentially the same results. The two straight lines correspond to excitation of the $v' = 1$ and $v' = 2$ levels with slopes corresponding to $\sigma_{01} = 1.26 \times 10^{-16}$ cm^2 and $\sigma_{02} = 0.299 \times 10^{-16}$ cm^2, respectively.

III. EXPERIMENTAL RESULTS AND DISCUSSION

Energy-loss spectra were obtained for the $H^+ + H_2$ system in the laboratory energy range 5–1500 eV and for the $D^+ + H_2$ system in the range 30–2500 eV. Elastic scattering results are presented in Table I and shown in Fig. 5. Figure 6 shows the increase of $I_{v'}$ as a function of energy. The measured values of the excitation cross sections are presented in Tables II and III and smoothed points are plotted in Figs. 7 and 8 as smooth curves. Such a presentation of the data is possible because of the close spacing of the experimental points (see Ta-

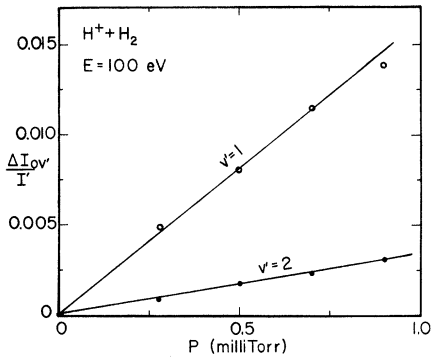

FIG. 4. Pressure dependence of proton-impact excitation to the $v' = 1$ and $v' = 2$ vibrational energy levels of H_2.

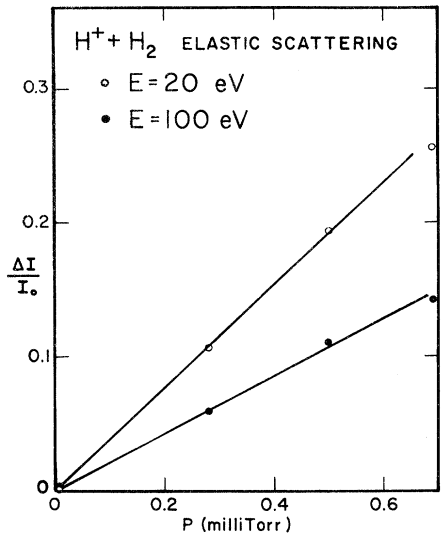

FIG. 5. Pressure dependence of elastic scattering of protons by H_2 at laboratory energies of 20 and 100 eV. This plot was obtained from the attenuation of the proton beam at various pressures of H_2 gas in the collision chamber.

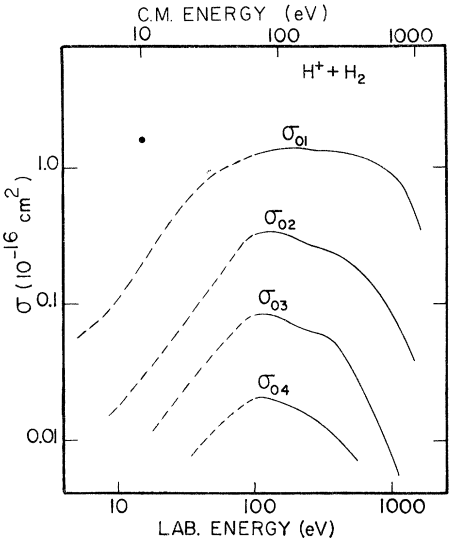

FIG. 7. H^+-H_2 vibrational excitation cross sections. The solid-line portion indicates total cross-section value, and the dashed line indicates partial cross section measured in the forward direction from $\Theta = 0°$ to $\Theta = 1.9°$. • is the cross section obtained from the relative differential cross sections of Udseth *et al.* (Ref. 21).

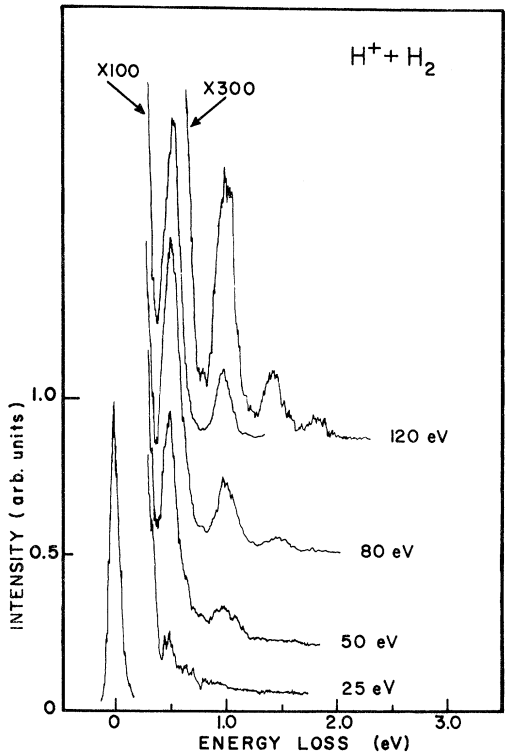

FIG. 6. Increase of vibrational excitation with ion energy. This superposition of energy-loss spectra taken at various energies shows the increase and onset of the vibrational excitation to the first four vibrational levels of H_2 by proton impact as the proton energy is increased from 25 to 120 eV. All curves, except the elastic peak and the curve marked ×300, are to be read as ×100.

bles II and III).

The data for the $H^+ + H_2$ system are the average of four complete runs while those for $D^+ + H_2$ are the average of only three. The deviations included next to the cross sections in Tables II and III indicate the scatter of the data.

The estimated error of measurement is approximately the same in both systems except for possible H_2^+ contamination of the D^+ beam. Since the cross section for vibrational excitation in the $H_2^+ + H_2$ system was below the limit of detectability of this experiment (that is, below about 5×10^{-19} cm^2), the effect of H_2^+ contamination would be to decrease the observed value of the cross section. A mass spectrum of the ion source output was obtained before every run, and this showed that, with D_2 gas in the ion source, the D^+ ion intensity was always more than 100 times the H^+ ion intensity; with H_2 gas at approximately the same pressure in the ion source, the H_2^+ ion intensity was about two times

TABLE I. Elastic scattering measurements. σ_a represents the elastic cross-section measurements by Cramer (see Ref. 18) with a minimum angle $\Theta_0 = 4.18°$, and σ_b represents the measurements made in this experiment with $\Theta_0 = 1.9°$.

E_{lab} (eV)	σ_a (10^{-16} cm^2)	σ_b (10^{-16} cm^2)
20	13.3	30.6
100	2.19	17.0
σ(20) eV)/σ(100 eV)	6.08	1.80

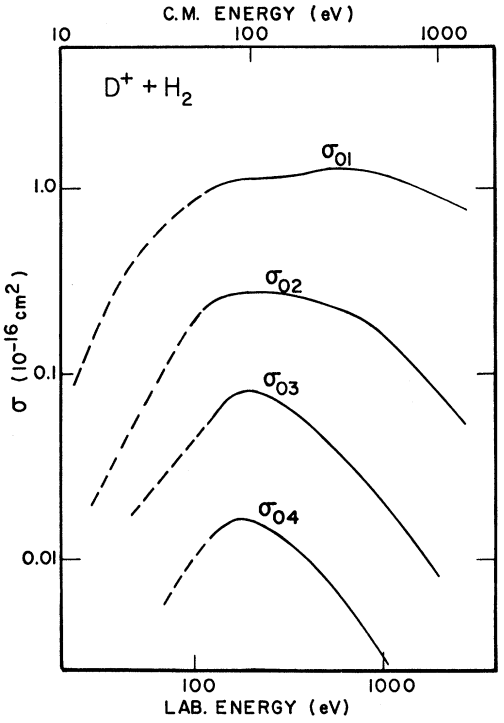

FIG. 8. $D^+ + H_2$ vibrational excitation cross section. The significance of the solid and dashed line portions is the same as in Fig. 7.

that of the H^+ intensity. Hence, the H_2^+ ion contamination of the D^+ beam is estimated to be not more than 2%.

The only calibration error in these measurements comes from the pressure measurement with the capacitance manometer. The error in using this instrument has been estimated at ± 5% of the calibration supplied by the manufacturer.[17] The error incurred in the determination of the current ratios entering Eq. (6) is determined by the deviations of the various electrometer amplifier gain settings from their stated values. This error was easily found to be less than ± 3%. With these figures, the estimated error of measurement of the cross sections reported in Tables II and III is ± 8%.

The system $D^+ + H_2$ was included in this study for two reasons. First, it was introduced as a further check of the experimental procedure. As expected, there were no observable effects of apparatus energy bias or distortion which might artificially influence the energy dependence of the cross sections. The cross sections for both systems were found to be similar only when considered as a function of the relative velocity of the colliding partners. The second reason for including the $D^+ + H_2$ system was to search for the effects of the isotope distortion of the H_3^+ potential surface of interaction on the transition probabilities for vibrational excitation.[8]

Although the apparatus slits were not chosen for measurements of elastic scattering, very reasonable elastic scattering cross sections were obtained from the primary-beam attenuation at energies below about 100 eV. These results are discussed in Sec. IIIA.

A. Elastic Scattering

Elastic scattering was measured in the $H^+ + H_2$ system at two laboratory energies: 20 and 100 eV.

TABLE II. $H^+ + H_2$ vibrational excitation cross sections for the first four vibrational levels of the electronic ground state of H_2. E represents the proton laboratory energy and $\sigma_{0v'}$ represents the cross section for excitation of the $0 \rightarrow v'$ transition.

E (eV)	σ_{01} (10^{-16} cm^2)	σ_{02} (10^{-16} cm^2)	σ_{03} (10^{-16} cm^2)	σ_{04} (10^{-16} cm^2)
5	0.076	0.014 ± 0.007		
10	0.111	0.026		
15	0.192	0.038		
20	0.304	0.038	0.014 ± 0.007	
25	0.408	0.045	0.024	
30	0.540 ± 0.031	0.060		
35	0.760	0.095	0.028	0.011 ± 0.005
40	0.698	0.095		
50	0.908	0.103	0.031	0.009
60	0.995	0.157		
70	1.05	0.260	0.070	0.015
80	1.09	0.290	0.110	
90	1.20	0.350	0.110	
100	1.26	0.299 ± 0.050	0.065	0.009
110	1.11	0.290	0.085	
120	1.11	0.316	0.066	0.021
130	1.26	0.330	0.070	0.020
140	1.32 ± 0.10	0.340	0.070	0.013
150	1.33	0.330	0.084 ± 0.015	0.019
160	1.23	0.320	0.057	
170	1.27	0.330	0.060	0.018
180	1.22	0.300	0.056	0.020 ± 0.005
190	1.37	0.320	0.065	0.018
200	1.28	0.300	0.051	0.017
225	1.19	0.230	0.044	0.010
250	1.32	0.240 ± 0.041	0.048	0.010
275	1.30	0.230	0.054	0.012
300	1.34	0.253	0.058	0.014
325	1.40 ± 0.12	0.230	0.064 ± 0.010	0.024
350	1.38	0.249	0.062	0.012
375	1.17	0.226	0.063	0.011
400	1.28	0.221 ± 0.043	0.057	0.011
425	1.26	0.210	0.041	0.015 ± 0.005
450	1.38	0.230	0.038	0.008
475	1.24	0.194	0.039 ± 0.010	
500	1.27 ± 0.12	0.182	0.029	
525	1.25	0.192	0.040	0.008
550	1.26	0.192	0.038	
575	1.26	0.185	0.031	
600	1.19	0.172	0.020	
650	1.08			
700	1.18	0.155 ± 0.033	0.019	
750	1.08			
800	1.10	0.124	0.015	
850	1.00 ± 0.10			
900	1.17	0.096	0.009 ± 0.005	
950	0.910			
1000	0.920	0.070	0.005	
1100	0.870	0.081		
1200	0.745	0.061 ± 0.030	0.006	
1300	0.700 ± 0.10	0.049		
1400	0.545			
1500	0.430			

TABLE III. $D^+ + H_2$ vibrational excitation cross sections for the first four vibrational levels of the electronic ground state of H_2. For notation see Table II.

E_{lab}(eV)	σ_{01} (10^{-16} cm^2)	σ_{02} (10^{-16} cm^2)	σ_{03} (10^{-16} cm^2)	σ_{04} (10^{-16} cm^2)
30	0.168 ± 0.038	0.010 ± 0.005		
35	0.193	0.039	0.015 ± 0.006	
40	0.331	0.039		
45	0.369	0.047	0.017	
50	0.412 ± 0.036	0.056		
55	0.492	0.069	0.030	
60	0.547	0.080 ± 0.020		
65	0.642	0.083	0.026	
70	0.604	0.178		
75	0.716			
80	0.727	0.094	0.018	0.006 ± 0.005
85	0.777	0.117	0.038 ± 0.008	0.013
90	0.741	0.182		
95	0.779	0.195	0.036	0.011
100	0.856 ± 0.050	0.235 ± 0.045	0.040	0.011
110	0.968	0.213	0.040	0.011
120	0.831	0.202	0.044	0.009
130	1.11	0.250	0.076	0.020
140	1.07	0.289	0.097	
150	1.08	0.262	0.071 ± 0.010	0.014 ± 0.005
160	1.16	0.312		
170	1.03	0.270	0.077	0.015
180	0.961 ± 0.052	0.209	0.058	0.014
190	1.00			
200	1.16	0.311 ± 0.051	0.076	
220	1.10	0.252	0.083	0.015
240	1.09	0.222	0.061	
260	1.15	0.325	0.079	0.010 ± 0.005
280	1.17	0.276	0.072 ± 0.010	
300	1.07	0.232	0.053	0.010
325	1.17	0.300	0.044	0.011
350		0.221 + 0.032	0.056	0.016
400	1.08 ± 0.10	0.188	0.070	0.015
450	1.33	0.231	0.040	
500	1.22	0.192	0.054	
600	1.28	0.182 ± 0.032	0.031 ± 0.010	0.005
700	1.48	0.231		
800	1.48 ± 0.12	0.230	0.035	0.005 ± 0.003
900	1.46			
1000	1.08	0.139	0.019	0.003
1200	1.00	0.110 ± 0.030	0.013	
1400	1.01 ± 0.10	0.105		
1600	0.980	0.089	0.010 ± 0.006	
1800	0.972	0.081	0.008	
2100	0.928	0.079		
2450	0.843 ± 0.10	0.061		

The attenuation of the primary beam was approximately constant for energies larger than 100 eV, although at high energies the principal cause of attenuation was charge transfer[18,19] rather than elastic scattering. Figure 5 shows the pressure dependence of the intensity lost from the primary beam due to elastic scattering. The elastic cross sections measured represent[20] $\sigma = 2\pi \int_{\theta_0}^{\pi} \sigma(\theta) \sin\theta \, d\theta$, where $\theta_0 = 1.9°$. In Table I, σ_b denotes the cross section for elastic scattering of H^+ by H_2 (not corrected for charge transfer) obtained from Fig. 5. σ_a denotes the corresponding results of Cramer.[18] θ_0 was 4.18° for the measurements reported by Cramer, so it is to be expected that the values reported here should be larger. The ratio $\sigma(20\text{ eV})/\sigma(100\text{ eV})$ differs markedly from the corresponding ratio in the work of Cramer, but this is not entirely unexpected in view of the general behavior of the differential scattering cross section at small angles. Udseth *et al.*[21] have recently observed the rainbow scattering in the $H^+ + H_2$ system at 10 eV (c.m.) energy. An inspection of their data indicates a rainbow angle χ_r of approximately 22° in the c.m. system. The kinetic energy E and the rainbow angle χ_r are related by the approximate relation

$$\chi_r = B(\epsilon/E), \tag{7}$$

where ϵ is the well depth of the potential of interaction and B is a constant which depends on the interaction potential.[22]

With the aid of Eq. (7) it is expected that $\chi_r = 3.3°$ (laboratory angle $\theta_r = 2.2°$) at $E = 67$ eV c.m. energy (100 eV lab energy). Udseth *et al.* have also observed a rainbow structure associated with vibrational excitation. (Implications with respect to this work will be discussed in Sec. III B.) Thus, it is expected that the differential cross section will increase very rapidly with decreasing angle in the neighborhood of $\theta \simeq 2°$ for a proton laboratory energy of about 100 eV. This rapid increase around $\theta \simeq 2°$ is what makes the cross section measured in this experiment at 100 eV much larger than Cramer's. In Cramer's measurement, the rainbow-scattered particles were not counted as elastic scattering at 100 eV because $\theta_0 = 4.18°$ for his measurement. Thus, the rainbow behavior of the cross section at 100 eV accounts for the discrepancy between the ratios in Table I.

B. Vibrational Excitation

Figure 6 shows four energy-loss spectra taken at four different energies. The primary beam intensity was approximately the same for all four, and the target-gas pressure was kept constant at 0.70 mTorr as the energy was varied. The increase of the cross sections and the onset of the excitation of the first four vibrational levels are clearly shown.

There is good reason to believe that there may be considerable rotational excitation accompanying vibrational excitation.[23] In this experiment, we looked for a change in the character of rotational excitation as a function of kinetic energy. Such an effect would appear as a shift of the energy-loss peaks with changing kinetic energy. There was a random shift of ± 0.015 eV in the location of the energy-loss peaks, so that a shift of the order of 0.030 eV should have been easily detected. Since the target gas is at room temperature, about 67% of the molecules populate the $J = 2$ rotational state.[10] Transitions from this state result in a minimum of 0.030 eV shift in energy for the $J = 2 \rightarrow J = 1$ transition, all other transitions giving larger shifts. No such shift was detected in this experiment, which indicates that the initial and final rotational states involved in the collision were the same at

all energies involved in this experiment.

The broadening of the vibrational peaks seen in Fig. 6 amounts to well over two times the primary-beam energy spread. This is observed at all energies, and it can be explained in terms of the recoil imparted to the target molecule upon collision with a proton.[1,20]

The cross sections for forward-scattered proton- and deuteron-impact excitation to the first four vibrational levels of H_2 are shown in Figs. 7 and 8, respectively.

The cone of acceptance of the detector has a half-angle of $\theta_0 = 1.9°$ as mentioned above, so the cross sections measured here are related to the differential scattering cross section by

$$\sigma_{0v'} = 2\pi \int_0^{\theta_0} \sigma_{0v'}(\theta) \sin\theta \, d\theta. \tag{8}$$

Because of the divergence of the beam at low energies, it was impossible to determine the angular distribution of elastically and inelastically scattered particles at the lower energies where wide-angle scattering is expected to become important. Thus, for energies below approximately 100 eV the measured cross sections for the proton-H_2 system are to be interpreted as partial cross sections and for energies above 100 eV they are to be interpreted as total cross sections. The corresponding energy for the $D^+ + H_2$ system occurs at approximately 130 eV.

Udseth *et al.* do not give absolute cross-section values. However, their observed relative cross sections can be used in conjunction with the inelastic cross sections measured here and the elastic cross sections of Cramer to give a rough estimate of the total cross section at 15 eV laboratory energy. A graphical integration based on their relative cross sections gives an estimate of $(1.8 \pm 0.5) \times 10^{-16}$ cm^2 for the total excitation cross section to the $v' = 1$ level at 15 eV laboratory energy. This value has been placed in Fig. 7 at the corresponding energy.

These results indicate that the maxima observed in Figs. 7 and 8 are to be interpreted as the points at which grazing collisions reach maximum efficiency in exciting vibrational transitions. The actual peaks of the complete total cross sections should occur at energies somewhat lower than those indicated in Figs. 7 and 8. Because of the large spread of the maxima in energy, the location of the maxima of the complete total cross section should be located close to but below the ones determined from Figs. 7 and 8. Thus, the energy values at the maxima observed in this experiment are upper bounds of the values corresponding to the complete total cross section. Figures 7 and 8 show that the maxima occur at successively lower energies as v' increases from 1 to 4. The velocities corresponding to the energy values at the maxima are tabulated in Table IV.

Since the energy of excitation is well defined in this process, it is expected that the adiabatic theory should give a qualitative prediction of the location of the maxima observed. Thus, the probability of excitation should be highest when the collision time τ_c is approximately equal to the period of vibration τ_v of the excited state. The collision time is given by

$$\tau_c = 2a/v \, , \tag{9}$$

where v is the relative velocity, and a, the collision length, is a distance corresponding to the range within which the perturbation of the H_2 energy levels is sufficient to induce a transition to a higher energy level. Table IV shows the values of a which were obtained using the above assumptions. These values of a are also to be considered as upper bounds for the collision distances corresponding to the total cross section; however, in view of the simple definition of the collision distance, it is more meaningful to interpret the collision distances in Table IV as those corresponding to grazing collisions in which the direction of motion is essentially undisturbed by the excitation collision.

In Table IV, $\Delta k/k$ is the fractional change in the spring constant of H_2 due to electron exchange with the incoming ion. These values have been obtained from the work of Korobkin and Slawsky,[24] who calculated the dilation of H_2 bond lengths due to electron exchange with a nearby proton. Slawsky and collaborators[24,25] propose that excitation occurs in two parts. In the adiabatic part of the collision the spring constant of the molecule is lowered by the approach of the ion. Excitation in the manifold of lowered vibrational energy levels then occurs at the moment of impact during the shorter diabatic

TABLE IV. Collision distance and vibrational-constant distortion. The velocities v corresponding to the maxima of the excitation cross sections are given for the first four vibrational levels. The quantity a denotes the collision distance associated with each velocity and $\Delta k/k$ gives the H_2 vibrational-spring-constant distortion induced by a proton approaching to within a distance a (Rev. 24).

v'	$v(10^7$ cm/sec)	a(Å)	$\Delta k/k$
	$H^+ + H_2$		
1	1.95	7.8	0
2	1.63	3.3	0.07
3	1.45	1.9	0.32
4	1.45	1.5	0.47
	$D^+ + H_2$		
1	2.39	9.6	0
2	1.38	2.8	0.09
3	1.34	1.8	0.37
4	1.29	1.3	0.54

part of the collision. The values of $\Delta k/k$ indicate the amount of the H_2 potential distortion necessary to reach the corresponding vibrational level by proton impact.

In view of the large spread in energy of the cross-section maxima, it is not unreasonable to assume that there is a range of collision distances corresponding to different collision lifetimes for each transition. Indeed, it has been shown[6] that the energy at which the probability of excitation reaches a maximum is strongly dependent on the impact parameter of the collision, with the larger impact parameters giving rise to excitation maxima at higher energies. This result and the results in Table IV give a qualitative understanding of the reason the cross sections for excitation to $v' \geq 2$ decrease more rapidly at the high energies than does that for $v' = 1$ (see Figs. 7–9). As seen from Table IV, transitions to the higher levels require a closer approach by the proton than do transitions to the lower levels. And, since only grazing collisions are being considered, it is apparent that only small values of the impact parameter lead to transitions to higher vibrational levels. This effect, and the fact that smaller impact parameters result in excitation maxima at lower energies, give rise to a more rapidly decreasing function of energy for the cross sections corresponding to the higher energy levels.

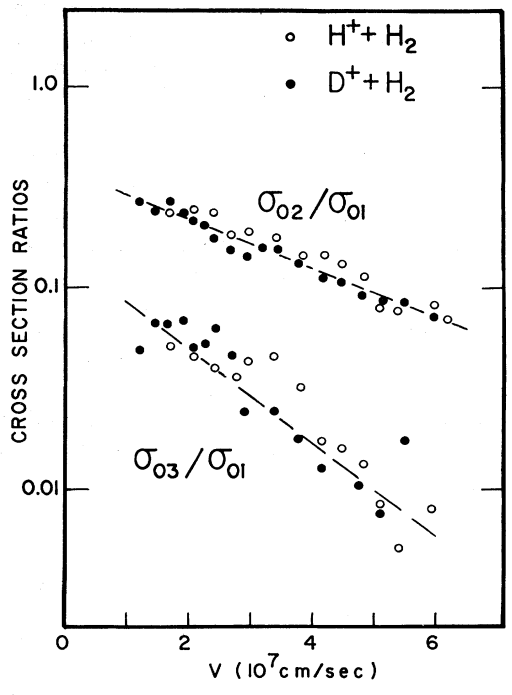

FIG. 9. Dependence of cross-section ratios on velocity for the $H^+ + H_2$ and $D^+ + H_2$ systems. The negative slopes indicate that excitation to the higher vibrational levels decreases more rapidly than excitation to the lower vibrational levels. The significance of this result is explained in the text. The isotope effect on the interaction potential does not lead to significant changes in the transition probabilities at these energies.

This is consistent with our results since it means that the transition probabilities for a given energy level, when averaged over a range of impact parameters, give rise to a net transition probability whose span in kinetic energy depends on the breadth of the range of impact parameters which is effective in inducing the transition. This range of impact parameters becomes smaller as the excitation energy increases. The wide spread of the maximum of σ_{01} in Figs. 7 and 8 indicates that excitation to the first level occurs over a very broad range of impact parameters, while the more rapid decrease of σ_{02}, σ_{03}, and σ_{04} indicates narrower and narrower ranges of impact parameters for excitation of higher levels. The effect is demonstrated very clearly in Fig. 9 where the ratios σ_{02}/σ_{01} and σ_{03}/σ_{01} are observed to decrease as the energy (velocity in this figure) increases.

An attempt was made to fit the data at the higher energies (> 100 eV) to the theoretical results of Shin.[6] This was done mainly in an effort to determine the behavior of the total cross section at lower energies (< 100 eV). As mentioned earlier, Shin's computations were carried out for a three dimensionally adapted Lennard-Jones potential. For an appropriate well depth of 2–4 eV,[9] it was found that the potential constant σ had to be in excess of 10×10^{-8} cm; this gives a potential minimum at distances larger than 10×10^{-8} cm, which is absurd since the expected value is less than 1×10^{-8} cm.[3] An examination of the formulas involved in this computation shows that the main features (location of maxima and magnitudes of slopes) of the cross section depend very strongly on the form of the potential. It is thus reasonable to expect that a potential could be found which would fit our data with this theory.

IV. CONCLUSIONS

The excitation cross sections reported here have contributed much to the understanding of the vibrational excitation process.

A comparison with vibrational excitation in larger diatomic molecules[11,12] reveals some very important differences. Vibrational excitation has been investigated in the systems $O_2^+ + Ar$, $O^+ + O_2$,[11] and $Ar^+ + D_2$.[12] On these systems, the excitation cross sections reach maxima at energies in the neighborhood of 20 eV or less, and multiquantum transitions become more important as the kinetic energy increases. The energy dependence of these transitions is in reasonable agreement with the semiclassical results of Shin which were calculated using a Lennard-Jones potential.[6] Of course, the well

depths of the interaction potentials in these systems are much smaller than the well depth for the proton-H_2 system, and because of the weaker interaction which is more like the interaction between uncharged particles, these larger systems are better described by a Lennard-Jones potential. A further consequence of the weaker interaction is that the molecular spring constant is perturbed much less than in the proton-H_2 system, and therefore the perturbation of the energy levels will not be very significant in inducing transitions.

Our experimental results are consistent with the adiabatic hypothesis[26] in that they give reasonable values for the collision distances of grazing encounters corresponding to the excitation of the first four vibrational energy levels of the electronic ground state of H_2. As expected from the decrease of vibrational period with increasing energy levels, the collision distances decrease with increasing energy levels. These results, viewed in the light of the calculations of Korobkin and Slawsky for the $H^+ + H_2$ system,[24] indicate that the proton must approach very close to the molecule to excite the higher vibrational levels. It is observed that, as a consequence of this requirement, the cross sections corresponding to the higher-energy levels must decrease more rapidly with increasing energy than those corresponding to the lower energy levels. This last conclusion is understood qualitatively in terms of the results obtained by Shin for the Lennard-Jones potential, as explained in Sec. III.

Apparently, the lack of quantitative agreement with Shin's calculation is due to the fact that no account is taken of the charge-induced dipole term in the interaction potential. This attractive term, with an r^{-4} dependence, would extend the range of interaction beyond that of the r^{-6} term in the Lennard-Jones potential, and would account for the large range of impact parameters involved in the excitation collisions observed here.

An extension of the importance of close range impact to the energy region below 100 eV would indicate that most of the forward scattering comes from the range of impact parameters where the deflection function for the classical trajectory passes from $\chi > 0$ (the positive branch) to $\chi < 0$ (the negative branch).[27] This region, which always occurs at impact parameters smaller than those corresponding to the rainbow region, is the one responsible for glory scattering in elastic collisions.[20,25] The proton-H_2 system provides an ideal case for the observation of glory scattering through the excitation channels since there is no interference from the primary beam. In the observation of elastic scattering in nonisotropic systems, such as $H^+ + H_2$, much information about the potential is lost because the observed rainbows are necessarily averages of collisions with different orientational configurations. It is hoped, however, that some of this information may be gained back by comparison of our results with theoretical calculations and also by a study of the forward glory scattering that is expected to arise in the inelastic channels at lower energies.

The excitation cross sections reported here clearly indicate that vibrational excitation must be a very important process in nature. At low energies (< 100 eV), the vibrational excitation cross section is much larger than the charge-transfer cross section, and at higher energies (> 300 eV),[13,14] it is of the same order of magnitude as elastic scattering. Furthermore, because of the large amount of energy (0.5 eV) lost per collision, it is obvious that vibrational excitation is more effective than elastic scattering in slowing down energetic particles. Thus, at high energies, vibrational excitation is expected to play the major role in determining the rate of energy dissipation; at lower energies, it will decreasingly compete with elastic scattering, and finally at energies below threshold (about 0.75 eV), only elastic scattering will determine the rate of energy dissipation. Hence, it is expected that vibrational excitation should play a very important role in the energetics of high-temperature plasma, and in the energy degradation of protons and other bare nuclei incident on the upper atmosphere as cosmic rays.

---

*Research supported by a grant from the National Science Foundation.

[1]J. H. Moore, Jr. and J. P. Doering, Phys. Rev. Letters 23, 584 (1969).

[2]F. H. M. Faisal, Phys. Rev. 4, 596 (1971).

[3]For two excellent reviews of the theory of excitation collisions the reader is referred to D. Rapp and T. Kassal, Chem. Rev. 69, 61 (1969), and K. Takayanagi, Progr. Theoret. Phys. (Kyoto) Suppl. 25, 1 (1963).

[4]C. F. Hansen and W. E. Pearson, J. Chem. Phys. 53, 3557 (1970).

[5]J. Liu, J. Chem. Phys. 53, 4567 (1970).

[6]H. K. Shin, J. Phys. Chem. 73, 4321 (1969).

[7]C. E. Treanor, J. Chem. Phys. 43, 532 (1965); 44, 2220 (1966).

[8]F. H. Mies, J. Chem. Phys. 42, 2709 (1965).

[9]R. E. Christoffersen, J. Chem. Phys. 41, 960 (1964); H. Conroy, *ibid.* 41, 1341 (1964); I. G. Csizmadia *et al.*, *ibid.* 52, 6205 (1970).

[10]G. Herzberg, *Spectra of Diatomic Molecules*, 2nd ed. (Van Nostrand, New York, 1950).

[11]P. C. Cosby and T. F. Moran, J. Chem. Phys. 52, 6157 (1970).

[12]T. F. Moran and P. C. Cosby, J. Chem. Phys. 51, 5724 (1969).

[13]J. H. Moore, Jr. and J. P. Doering, J. Chem. Phys. 52, 1692 (1970).

[14]The electron multiplier used here is a 20-dynode focused-mesh multiplier enclosed in a metallic cylinder. In order to measure the absolute current arriving at the

first dynode, the entire multiplier was isolated completely from earth ground, and the first dynode was connected directly to the electrometer. The metallic cylinder containing the multiplier was biased with a negative potential with respect to the multiplier. The same electrometer that was used to measure the ion current in the collision chamber was used with the multiplier. However, as shown in Fig. 2, the transmission ratio measured was always $1.1 < T < 1.2$ for "100%" transmission. This indicates that secondary electron suppression was not as good in the electron multiplier measurement as it was in the collision chamber.

[15]A. Papoulis, *Systems and Transforms with Applications in Optics* (McGraw-Hill, New York, 1968).

[16]P. A. Sturrock, *Static and Dynamic Electron Optics* (Cambridge U.P., Cambridge, 1955).

[17]S. Ruthberg, Natl. Bur. Std. (private communication).

[18]W. H. Cramer, J. Chem. Phys. 35, 836 (1961).

[19]D. W. Koopman, Phys. Rev. 154, 79 (1967).

[20]E. W. McDaniel, *Collisional Phenomena in Ionized Gases* (Wiley, New York, 1964).

[21]H. Udseth, C. F. Giese, and W. R. Gentry, J. Chem. Phys. 54, 3642 (1971).

[22]The relation $\chi_r = B(\epsilon/E)$ has been found to be valid on the basis of theoretical and experimental evidence for $\chi_r \lesssim 90°$. Furthermore, it is quite evident that the constant B is relatively insensitive to changes in the interaction well depth ϵ, and that with χ_r in degrees, the constant $B \simeq 115 \pm 15$ for both ion-neutral and neutral-neutral interactions. For theoretical results on χ_r, see E. A. Mason, J. Chem. Phys. 26, 667 (1957), and E. A. Mason, R. J. Munn, and F. J. Smith, J. Chem. Phys. 44, 1967 (1966). For experimental results on ion-neutral interactions, see F. A. Herrero, E. M. Nemeth, and T. L. Bailey, J. Chem. Phys. 50, 4591 (1969), and R. L. Champion *et al.*, Phys. Rev. A 2, 2327 (1970). For experimental results on neutral-neutral interactions, see F. A. Morse and R. B. Bernstein, J. Chem. Phys. 37, 2019 (1962), and D. Beck, J. Chem. Phys. 37, 2884 (1962). Adopting a value of $B = 115$, we obtain $\epsilon \simeq 2$ eV for the average well depth of the anisotropic interaction of H^+-H_2.

[23]J. H. Moore, Jr. and J. P. Doering, Phys. Rev. 174, 178 (1968).

[24]J. Korobkin and Z. I. Slawsky, J. Chem. Phys. 37, 226 (1962).

[25]F. W. DeWette and Z. I. Slawsky, Physics 20, 1169 (1954).

[26]H. S. W. Massey, Rept. Progr. Phys. 12, 248 (1948–49); E. Gerjuoy, Rev. Mod. Phys. 33, 544 (1961).

[27]K. W. Ford and J. A. Wheeler, Ann. Phys. (N.Y.) 7, 259 (1959).

PHYSICAL REVIEW A VOLUME 5, NUMBER 2 FEBRUARY 1972

Measurements of Energy and Angular Distributions of Secondary Electrons Produced in Electron-Impact Ionization of Helium*

W. K. Peterson,† E. C. Beaty,‡ and C. B. Opal§
Joint Institute for Laboratory Astrophysics, University of Colorado, Boulder, Colorado 80302
(Received 27 September 1971)

The energy and angular distributions of electrons produced in the ionization of helium by electrons with energies between 100 eV and 2 keV have been measured in a crossed-beam apparatus consisting of a fixed hemispherical energy analyzer and a rotatable electron gun. Distributions of secondary electrons (those electrons departing with energies less than one-half that of the incident primary electrons) were obtained for a wide range of energies and for angles between 30° and 150° with respect to the direction of the incident primary electron beam. The observed angular distributions were significantly different from the results of two early electron-impact measurements; however, they agreed to the extent expected with more recent results and with similar proton-impact data. For secondary energies above about 50 eV and for primary energies greater than 300 eV, the energy distributions (the cross sections integrated over angle) were observed to be very nearly equal to the distribution given by the Mott formula for free-electron–free-electron scattering multiplied by the number of electrons in the target.

I. INTRODUCTION

Cross sections for the production of low-energy electrons ejected in electron-impact ionization by fast electrons are of importance in plasma physics, atmospheric physics, and radiation chemistry. In particular, since electron-impact excitation and ionization cross sections are largest in the energy range 20–200 eV for most atomic and molecular species, knowledge of the rate of production of secondary electrons in this energy range by high-energy electron-impact ionization is essential to an understanding of the total energy deposition by fast particles. Relatively little has been published about these cross sections. In a previous short note,[1] we reported measurements of the energy distribution of secondary electrons produced in electron-impact ionization of helium and compared the results to Born-approximation calculations. In this paper we give a more complete account of the experimental procedure and discuss in greater detail the observed energy and angular distributions.[2]

The quantity we have measured is the doubly differential cross section [called $\sigma(E_p, E_s, \theta)$ and ex-